Springer

KSME

Journal of Mechanical Science and Technology 28 (11) (2014) 4475~4482
www.springerlink.com/content/1738-494x
DOI 10.1007/s12206-014-1015-4

Numerical study of 2024 T3 aluminum plates subjected to impact and perforation †

Mohd Norihan Ibrahim[1,*], Waluyo Adi Siswanto[1] and Ahmad Mujahid Ahmad Zaidi[2]

[1]*Department of Engineering Mechanics, Faculty of Mechanical and Manufacturing Engineering, Universiti Tun Hussein Onn Malaysia, 86400 Parit Raja, Batu Pahat, Johor, Malaysia*
[2]*Department of Mechanical Engineering, Faculty of Engineering, Universiti Pertahanan Nasional Malaysia, Malaysia*

(Manuscript Received January 15, 2014; Revised June 5, 2014; Accepted July 2, 2014)

Abstract

The paper describes a work focused on the process of perforation of aluminum sheet. A numerical investigation has been carried out to analyze in details the perforation process subjected to normal impact by different nose shapes of projectiles. The perforation process has been simulated by the application of 3D analysis using IMPACT dynamic FE program suite. The comparison on failure modes depending on the projectile nose shape have been studied and evaluated. An appropriate constitutive relation was applied to describe the material behavior of the aluminum sheet. The study covered different failure modes including petalling, plug ejection and circumference necking of perforated aluminum sheet according to different level of impact velocity ranging from 100 m/s to 600 m/s. In this investigation, a special attention will be given on the deformation and failure.

Keywords: Finite element method; Projectile impact; Perforation; Failure mode

1. Introduction

The effect of local impact and global structural response may be involved in the perforation of a ductile plate subjected to the strike of a non-deformable projectile. The response of materials under dynamic loading has a considerable interest especially involving the perforation and penetration resulting from the impact of non-deformable projectiles and metallic plate. The deformation and the damage development in the target are relevant phenomena which should be considered when assessing the performance of aluminum sheets against impact loading.

Many publications can be found in the international literature dealing with high strain rate behavior of metallic materials related with different engineering applications [1, 2]. The deformation and the damage development in the target are relevant phenomena which should be considered when assessing the performance of aluminum sheets against impact loading. The perforation is dominated by the local penetration although the failure mechanism of the final perforation also influences the ballistic limit of a thick target, which depends on the target material, target dimensions, projectile nose and impact velocity.

A three dimensional model is developed in LS-DYNA/ explicit to simulate the perforation of steel and aluminum target using a Modified Johnson Cook model [3]. The numerical results show good correlation with the published experimental results and the study demonstrates that the material model is able to emulate failure characteristics of the steel and aluminum plates as observed in various experimental observations.

An analytical perforation model based on the cylindrical cavity expansion has been reformulated and used to calculate the ballistic perforation of resistance of the aluminum plates. The target material was modeled with the modified Johnson and Cook constitutive relation using constant strain 2D axisymmetric elements and adaptive rezoning. The physical behavior of the target during perforation is well captured in the FE simulations when the model is used [4].

Three dimensional numerical simulation using ABAQUS/ Explicit finite element code was carried out to study the effect of projectile nose shape on the ballistic resistance of ductile target by Iqbal et al. [5]. 1mm thick 1100-H12 aluminum targets were impacted by 19 mm diameter of blunt and hemispherical nosed projectiles. The projectiles with blunt nosed failed the target through shear plugging, imparting significant but more localized plastic deformation. The projectiles with hemispherical nosed caused stretching and thinning of target material resulting in huge local and global deformation. Further movement of projectile caused formation of irregular petals.

Iqbal et al. [6] also performed experimental and numerical simulation to study the failure modes and ballistic resistance

*Corresponding author. Tel.: +60 74537726, Fax.: +60 74536080
E-mail address: mnrihan7012@gmail.com
† Recommended by Associate Editor Chang-Wan Kim

of aluminum targets subjected to normal impact of doubled nosed projectiles such as conico-blunt, blunt-blunt and blunt-conico. The ABAQUS/Explicit finite element code was carried out to perform numerical simulation. The blunt-blunt projectile failed the target through plug formation. Two different plugs were removed from the target. The first plug was created due to the impact of the first blunt nose and the second plug by the second blunt nose of projectile.

Based on the experimental investigation, four stage models developed for the perforation of stiffened plate [7]. The four stages in the model are plug formation, dishing formation, petal formation and projectile exit. In this investigation, the analysis of process requires the following assumptions: (a) the amount of energy absorbed by the projectile is neglected, (b) the projectile move with the same velocity after the initiation of perforation, (c) the plastic deformation is taken into account in the target plate while elastic deformation is neglected and (d) the strain rate effect of the material is considered.

It is still a challenge to obtain a general structural model of perforation analysis, which incorporates the local failure analysis in the rigid-plastic model because different local response and failure modes, such as dishing, petalling or penetration, may appear for different plate thicknesses and impact velocity. The current paper presents the results of numerical investigation undertaken to study the perforation process of circular shape of target plate when subjected to the impact by different projectile nose shape at different velocity. The perforation capabilities of projectile against constraints plates were explored for an efficient damage and failure modes.

2. Numerical modeling

2.1 Finite element model

The proposed finite element model of projectiles is shown in Fig. 1. The projectile has the diameter of 22 mm for all types of nose shape. The circular shape of target plate has the diameter of 50 mm and 2 mm thickness. Both projectiles and target plate is modeled using finite element pre-processor GiD with IMPACT interface module. The plate is constrained around the edges and subjected to impact by a projectile with 22 mm diameter with multiple nose shape at different velocities. The projectile is modeled as contact triangle (CT) elements. Both the target plate and the projectiles are modeled in full so as to be able to simulate the failure mode in target plate from the point of impact towards the constraints edge and back.

A 3D finite element model for the simulation of the penetration process was developed in IMPACT explicit finite element program suite. The ability of the application programs in dealing with contact algorithms provide a powerful platform to simulate several types of armor target subjected to the impact of projectiles moving at various velocities [8]. The circular target plate is considered as deformable body and represented by the element mesh defined by triangle elements with the element mesh generated equal to 2.5. The elements, name as

Table 1. Material properties of target plate.

Type of material	Aluminum 2024 T3
Property of material	Elastoplastic
Young modulus, E	73.08 GPa
Poisson ratio, ν	0.33
Mass density, ρ	2700 kg/m^3
Thickness of plate	*2 mm*
Integration point	*5*
Yield stress, σ_y	0.35 GPa
Hardening factor	0.1
Contact type	Basic
Contact factor	10.00
Contact friction	0.25
Type of failure	Failure strain, $f = 0.50$

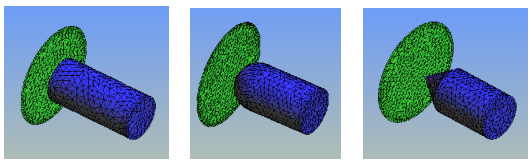

(a) (b) (c)

Fig. 1. Finite element model of projectiles and target plate: (a) blunt projectile; (b) hemispherical projectile; (c) conical projectile.

SHELL _C0_3 is three node shell elements based on the classical C0 formulation by Belytschko et al. [9]. The target plate may be divided into two region namely inner and outer region. Both inner and outer region represented by structured mesh defined by triangular element of SHELL _C0_3. The inner region represent on the central impact part while the outer region located sufficiently far from the impact zone does not show significant effect of deformation. The projectile is assumed as a rigid body and is categorized as contact triangle element. This assumption reduces the computational time required for the simulation.

An aluminum 2024 T3 is used as a material model of circular target plate. Aluminum 2024 T3 is a strain rate dependent isotropic elastic plastic model. The material properties of aluminum 2024 T3 is shown in Table 1. The material model in IMPACT dynamic FE program suite, aluminum 2024 T3 is examined for its suitability in simulating target plate under dynamic impact loading.

2.2 Constitutive relation

In a mathematical description of material behavior, the response of the material is categorized by a constitutive equation which gives the stress as a function of the deformation history of the body. The impact between projectile and target plate involve the development of permanent strain called plastic materials. A theory of contact deformation can be used to relate normal contact force to deformation and subsequently to

relate deformation to work done on the contact region by the normal force of colliding bodies.

In this research, a rigid 3-dimensional of projectile colliding against an elastic-plastic target plate and a nonlinear explicit 3-dimensional finite element program, IMPACT used to analyze the problem. In the elastic-plastic contact, the transition between perfectly-elastic and fully-plastic behavior can be based on the stress field due to expansion of a cylindrical or spherical cavity in an elastic-plastic solid [10]. The half-space contains a hydrostatic core of radius a surrounded by a cylindrical elastic-plastic shell of outer radius c which is centered at the initial point of contact. By performing an appropriate analysis, the mean contact pressure is obtained for the cylindrical cavity model as

$$\frac{p}{\sigma_y} = \frac{2}{3} + \frac{1}{\sqrt{3}}\left[\frac{4}{3\pi}\frac{Ea}{\sigma_y R}\right] \tag{1}$$

where p is the mean or average contact pressure, σ_y is the yield stress, E is the Young's Modulus, a is the contact patch and R is the radius of curvature. Through the process of substitution and evaluation on Eq. (1), the normal force F may be expressed as

$$\frac{F}{F_y} = \frac{a}{a_y}\left(1 + \frac{3}{3\sqrt{3}}\ln\frac{a}{a_y}\right) \tag{2}$$

the compliance relation for the elastic-plastic indentation during compressive stage of impact may be obtained as

$$\frac{F}{F_y} = \left[\frac{\delta_y}{\delta_y^2}\left(\frac{\delta}{\delta_y} - 1\right) + 1\right]^{1/2}\left\{1 + \frac{1}{3\sqrt{3}}\ln\left[\frac{\delta_y R}{a_y^2}\left(\frac{\delta}{\delta_y} - 1\right) + 1\right]\right\}. \tag{3}$$

The Lagrangian formulation is adopted to formulate the material constitutive relationship for dynamical characterization and deformation of target plate. Belytschko et al. [9] reported that the Lagrangian finite elements prove extremely useful in large deformation problems in solid mechanics and are most widely used in solid mechanics. The formulations apply to large deformations and nonlinear materials where they consider both geometric and material nonlinearities.

2.3 Failure criterion

The application of failure criterion on the material deformation behavior is widely accepted in the analysis of metallic structure subject to dynamic loading [2]. The material failure is defined by a constant value of the equivalent plastic strain. Since the target is very thin, the stress field across the thickness of the plate is nearly constant during the perforation process where the pressure along the projectile and plate interaction is constant. The value of failure strain adopted in the simulations, $f = 0.50$, which is estimated from the experimental observations of the material deformation behavior. This value is corresponding to the necking strain under dynamic loading. Lesuer [11] performed the evaluation of high strain rate, large strain deformation and fracture response using split Hopkinson pressure bar technique. The process of strain localization and necking formation that cause perforation of target plate is sufficiently defines in the finite element simulation.

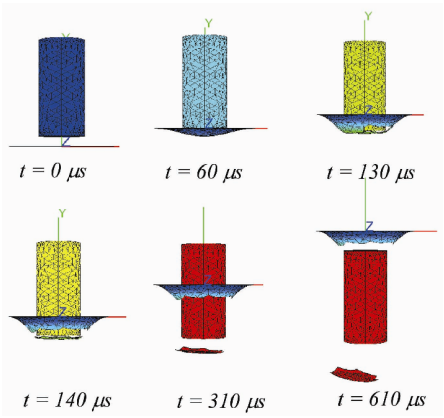

Fig. 2. Simulation of projectile impact at different time step control, t.

3. Result and discussion

In this section, an IMPACT/Explicit dynamic finite element code is used to simulate the penetration and perforation process. The failure process of aluminum plate when subjected to normal impact of projectile nose shapes were examined. There are several parameters affect the deformation and penetration of aluminum target plate when subjected to the impact by a projectile. Some of these parameters are the penetration process, petalling process, velocity impact, stress and strain rate effect and hole expansion.

3.1 Influence of time step control

At the time step, $t = 0$ μs, the blunt nose projectile remain in it rest position and the thin target plate made of aluminum is located 5 mm from the projectile as shown in Fig. 2. The dark blue color of projectile represents on the static position and no motion occurs. At time step, $t = 60$ μs, the projectile at the velocity of 100 m/s start impacting the circular target plate and through the initial impact, it is shown that initial deformation occur in form of concave shape and also called as dishing.

The deformation of impacted thin plate continued until it reaches the condition where the shell is undergoing plastic strain deformation and the initial crack progression observed. A little motion forward during impact phase leads to initial crack propagation around the blunt nose shape of projectile as shown at time step control, $t = 130$ μs.

At the time step $t = 140$ μs, necking process occurs and at the end plug ejected from the circular target plate. As the projectile move forward, the plug ejection fly simultaneously as the projectile move forwards as shown at time step control $t =$

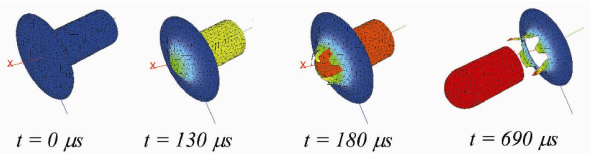

Fig. 3. Numerical results of hemispherical projectile configuration at impact speed of 100 m/s.

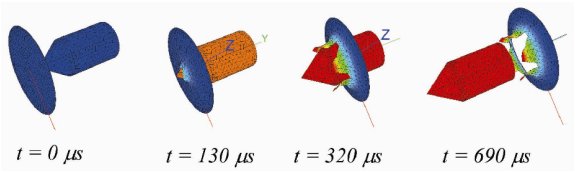

Fig. 4. Numerical results of conical projectile configuration at impact speed of 100 m/s.

310 μs and t = 610 μs respectively. The permanent plastic deformation will remain in its state once the projectile exiting fully the impacted zone. The processing time took 133182 ms.

3.2 Petalling process analysis

Fig. 3 shows the numerical results of hemispherical projectile in three dimensional (3D) configurations. At the time step, t = 130 μs, dishing formation occurs and the following motion of projectile leads to the crack propagation of the impacted surface and initial stage of perforation occurs at the speed of 180 μs. At the time step, t = 310 μs, half of the projectile body pass through the perforated surface and the petal formation generated around it. The beginning of the petalling process during perforation is always associated with fracture initiation and the outward move of petals as perforation continues. The petals generated in forms of uniform triangular cross section and some in forms of trapezoidal shape. When the time step reach at t = 690 μs, the projectile is exiting the perforated surface and through the observation made, there are five petals generated. The solving took 161792 ms.

The same phase of perforation process occurs on the projectile with conical nose shape impacting circular target plate as shown in Fig. 4. The formation of petals may be observed clearly at the time step, t = 320 μs, 580 μs, 690 μs where several number of petals formed with triangular and trapezoidal shape cross section. Anyhow, the effect of impact on the different shape of projectile nose shape yields different initiation of crack propagation pattern. The processing time took 248361 ms.

3.3 Plugging process analysis

Fig. 5 shows the numerical results of blunt projectile in three dimensional (3D) configurations. At the time step, t = 100 μs, dishing formation occurs and the following motion of projectile leads to the crack propagation. At the time step, t =

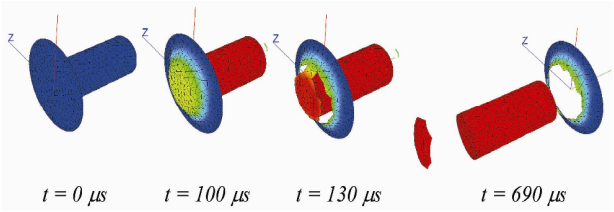

Fig. 5. Numerical results of blunt projectile configuration at impact speed of 100 m/s.

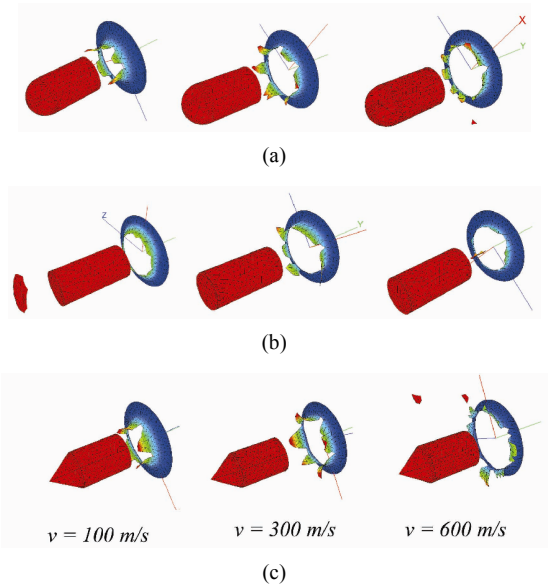

Fig. 6. Failure mode configuration of impacted target plate by different velocity impact: (a) hemispherical; (b) blunt; (c) conical.

130 μs, the projectile body perforate the surface and the plug formation generated. When the time step reach at t = 690 μs, the projectile is exiting the perforated surface with the plug fly forward as the projectile move. Therefore the blunt projectile failed the target through plug formation. This is due to the fact that impact of blunt nose shape of projectiles imparted an impulse to the indented area of the respective plates causing the ejected plugs with relatively small masses to accelerate. Comparison to all of projectile nose shape will eventually bring to concise and remarkable results where the projectile nose shape will significantly influence on the failure mode profile and pattern.

3.4 Influence of impact speed

Fig. 6 shows the failure mode yield through the penetration process of projectile towards thin aluminum target plate at three different speed impact of multiple shape of projectile nose shape. For the projectile impacting target plate at the speed of 100 m/s, the formation of petal observed explicitly for hemispherical and conical nose projectile. The develop-

ment of circumferential deformation leads to the crack propagation around the impacting surface. Different scenario occurs for blunt projectile impact where it failed the target through plug formation. The plug was created due to the impact of blunt nose projectile and it has circular and flat with diameter approximately equal to that of front nose.

At the speed of 300 m/s, the impact shows on the increment of the number of crack propagation around impacted surface for all type of projectile nose shape. The number of petal formation also increases for both hemispherical and conical projectile impact. Another effect detected is holes expansion. The perforation at the speed of 300 m/s contribute significantly on the hole enlargement for all type of projectile nose shape as shown in Fig. 6.

To further investigate on the influence of impact, the numerical simulation of the perforation process is proceeded with the impact of projectiles into target plate at the velocity of v = 600 m/s. For hemispherical projectile impact, the perforation of impacted target plate indicates multiple crack propagation and the formation of several plug fragmentation and holes enlargement process. The same scenario also occurs for the blunt and conical nose projectile impact. This is due to the large forced imposed on the impacted surface area.

The influence of impact velocity on the failure mode may be observed explicitly with the enhancement of speed of projectile. The number of radial crack increases with the increase of impact velocity. This phenomenon is induced by the increase of circumferential strain level responsible of the crack initiation and progression [12, 13]. This is caused by the increase of the kinetic energy transferred to the material of the target when the impact velocity increases. Although the number of cracks is larger in case of high impact velocity, the failure mode induced by necking that appears in this situation reduces the size of the petals.

3.5 Holes enlargement analysis

The effects of speed on the enlargement of hole after impact are shown in Figs. 7 and 8. The images shows the post perforation of conical nose shape of projectile impacting circular target plate at the velocity ranging from 100 m/s, 300 m/s and 600 m/s, respectively. The top images in row illustrates the gap yield between the projectile and perforated surface while the bottom images in row indicates the size of hole enlargement for all velocity impact.

The failure mode obtained for impacted target plate is varies in terms of crack propagation, petal formation and the size of holes expansion. Basically the crack propagation increases as the impact velocity increases. Similarly to the formation of petals where it increase when the impact speed increases and at certain impact velocity it reduces significantly on the size of petals. The enlargement of hole keeps increasing as the increase of velocity impact. At the velocity of v = 600 m/s the enlargement of holes increases, multiple cracks perforation exists and the plug ejection occurs.

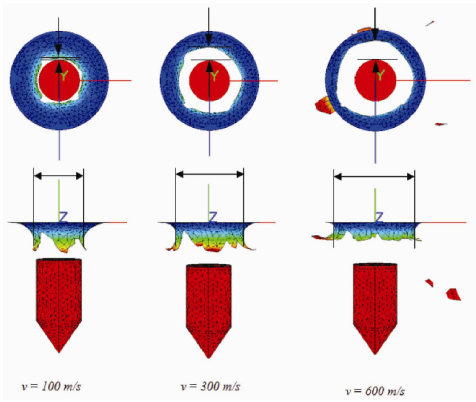

Fig. 7. Holes enlargement due the effect of velocity impact.

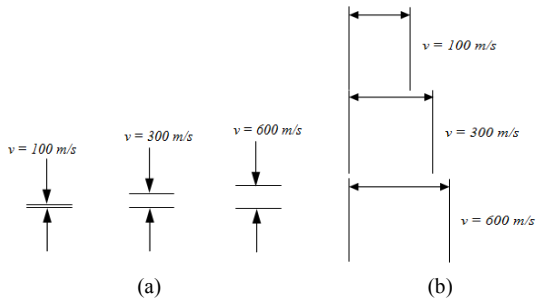

Fig. 8. Holes expansion process: (a) gap enlargement of projectile-target; (b) hole enlargement at different speed impact.

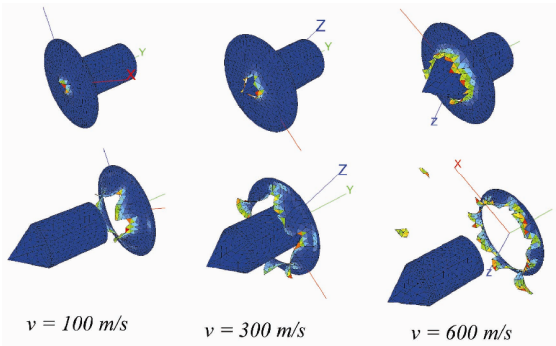

Fig. 9. Failure mode configuration of impacted target plate at different velocity impact.

3.6 Local strain effect on perforated surface

Fig. 9 shows the contour plot of failure mode which represent the strain occur in the direction of the motion of conical projectile impacting the target plate at different range of velocity impact. The images show that the perforated target region exhibit different tone of strain level. The highest strain is labeled with red color and its color tone decreasing as the strain level decreases. The portion of the target plate that was in contact with the projectile bent in the shape of projectile motion and crack apart to form petals. The maximum strain effect occurs when the plastic deformation takes place and the deformed surface start form initial crack propagation.

For the impact velocity of 100 m/s, the local strain reach the

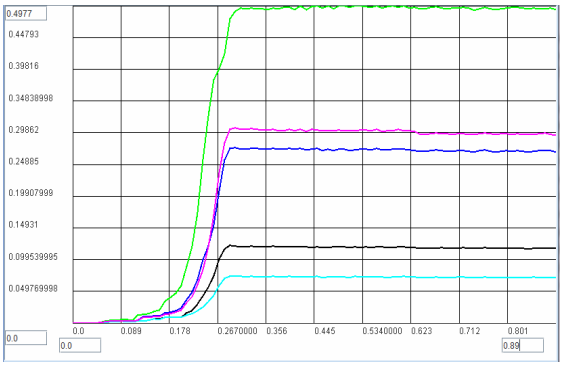

Fig. 10. Strain relative to time step, t for the impact velocity of 100 m/s.

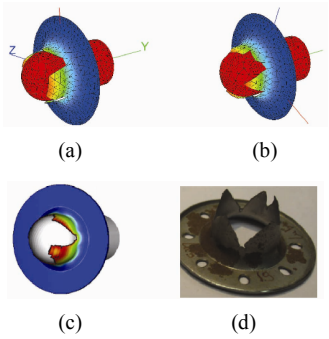

Fig. 11. Failure modes contour plots of the perforation process by hemispherical nose projectile impact: (a) numerical by IMPACT (AL 2024 T3); (b) numerical by IMPACT (steel ANSI C1020); (c) numerical by ABAQUS (mild steel ES sheet); (d) experimental (mild steel ES sheet).

maximum level at 0.498 (denoted with dark red for perforated target plate image) and its occur at the time step between 120 μs to 350 μs as shown in Fig. 10 (plotted in green line). At v = 300 m/s, local strain reach the maximum level at 0.498 (denoted with dark red) and its occur at the time step between 15 μs to 30 μs while at v = 600 m/s, local strain reach the maximum level at 0.498 (denoted with dark red) and its occur at the time step between 10 μs to 20 μs.

4. Comparison and verification

Finite element simulations have been performed using the explicit solution technique of the IMPACT finite element code. Simulations were carried out at different nose shape of projectile and at different velocities of impact. Comparison with others numerical and experimental results was done in order to validate on the accuracy and reliability of the results obtained using IMPACT dynamic finite element program suite. The focus area is on the profile of failure mode yield by different types of numerical simulation and also experimental finding.

4.1 Hemispherical nose projectile

Fig. 11(a) shows the failure modes contour plot for the impact between hemispherical projectile and thin aluminum 2024 T3 at the velocity of 40 m/s. When projectile move forwards and penetrating target plate, the progression of crack and failure leads to the formation of petals for aluminum target plate. The same phenomena also occur for the projectile-target interaction made of steel ANSI C1020 where the failed target indicates the formation of petals around the perforated surface (Fig. 11(b)).

In order to verify on the profile of failures, the similar geometry and dimensions of projectile and target plate was done by Rusinek et al. [12] as shown in Fig. 11(c) where the material used is made of mild steel sheets and using ABAQUS Explicit FE software to simulate the impact. Based on the analysis carried out, necking, radial cracking and petals formation are observed for the numerical result for both IMPACT and ABAQUS Explicit FE software.

The verification on the reliability of numerical finding also compared with the experimental analysis done by Rusinek et al. [12] as shown in Fig. 11(d). During the perforation, an enhancement of friction effect between the projectile and target plate leads to the strain localization and failure on the impacted surface. The perforated surface yields formation of petals similar to IMPACT and ABAQUS Explicit Finite Element program suite. Therefore, the formations of petals at the velocity of 40 m/s for hemispherical projectiles are in good agreement with between numerical results of IMPACT and ABAQUS as well as between IMPACT Explicit FE and experimental results.

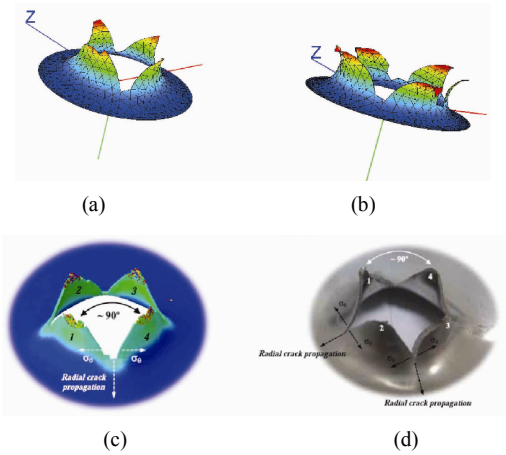

Fig. 12. Failure modes contour plots of the perforation process by conical nose projectile impact: (a) numerical by IMPACT (AL 2024 T3); (b) numerical by IMPACT (steel ANSI C1020); (c) numerical by ABAQUS (AISI 304 steel sheet); (d) experimental (AISI 304 steel sheet).

4.2 Conical nose projectile

Fig. 12 shows failure modes contour plots of the perforation process by conical nose projectile impact. Figs. 12(a) and (b) shows the failure modes obtained by conical nose projectile

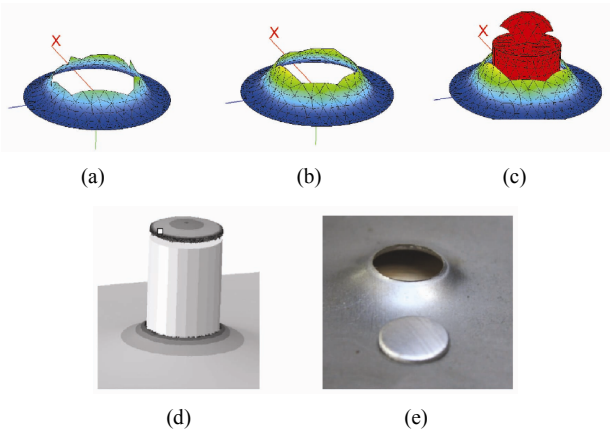

Fig. 13. Failure modes contour plots of the perforation process by blunt nose projectile impact: (a) Numerical by IMPACT (AL 2024 T3); (b), (c) numerical by IMPACT (Steel ANSI C1020); (d) numerical by ABAQUS (maraging steel sheet); (e) experimental (maraging steel sheet).

impacting circular aluminum 2024 T3 and steel ANSI C1020 target plate at the velocity v= 176.06 m/s respectively. Through the simulation of the impacted target plate, it is shown that the perforated target plate yield the formation of petals. The other analysis done by Rodriguez-Martinez [2] also illustrates the similar outcome but slightly different in terms of number of petals generation.

4.3 Blunt nose projectile

A more detailed study on the effect of projectile nose shape on the process of perforation has been made. The next comparison and verification is for the blunt nose shape projectile impacting circular aluminum target plate at the velocity of v = 141 m/s. Figs. 13(a)-(c) shows three dimensional failure modes contour plots of the perforation process by blunt nose projectile impacting circular target plate made of aluminum 2024 T3 and steel ANSI C1020, respectively. The failure modes of the steel sheet found that the projectile nose shape has a strong effect on the process of failure. It indicates that at the impact velocity of v = 141 m/s, a process of high speed cutting due to high shearing is observed inducing plug ejection as shown in Fig. 13(c).

The verification on the profile of failure and perforation pattern was done by comparing the outcome obtained by Kpenyigba et al. [14] as shown in Figs. 13(d) and (e), respectively. Based on the analysis carried out the failed target plate is due to the plug ejection of perforated surface for the simulation produced by IMPACT explicit finite element code and ABAQUS explicit finite element code. The numerical simulation also compared with the experimental analysis on the process of failure. Thus it is clearly observed that plug ejection are found to be in a good agreement between numerical simulation by IMPACT and ABAQUS finite element code as well as experimental analysis.

5. Conclusions

As observed in this work, the failure mode of the sheet aluminum used is strongly correlated to the projectile shape. Numerical simulations have been performed using Impact/Explicit finite element code. The numerical model allows for prediction of accurate impact failure mode depending on the projectile nose shape. Good agreement is found between numerical and experimental results done by other researchers and the FE simulations in terms of profile of failure. An aluminum circular target plates was impacted by several nose shape of projectiles of 22 mm diameter at various impact velocities. The effect of time step control, geometry shape, petalling process, plugging, impact speed, holes enlargement and the local strain on the deformation and ballistic behavior were studied. Based on the numerical observations, the following conclusions are drawn:

(1) The impact region of circular target plate is significantly affected by the projectile nose shape. The blunt nose projectile impact leads to the plug ejection of impact region while hemispherical and conical nose shape of projectile impact leads to the formation of petals around the perforated surface.

(2) The time step size play an important role in the stability of numerical analysis. The appropriate setting of time step control may provide remarkable influence on the processing time and duration of simulation. Thus the time step control contributes to the accurate of step by step deformation process and failure process of projectile impact towards target plate.

(3) The impact by using hemispherical and conical nose shape of projectile towards circular target plate leads to the formation of petals around the perforated surface. The conical nose projectile represents the failure mode by petalling due to the process of piercing while the hemispherical nose projectile form petalling due to the radial crack propagation during penetration.

(4) The blunt projectile failed the target through plug formation. This is due to the fact that impact of blunt nose shape of projectiles imparted an impulse to the indented area of the respective plates causing the ejected plugs with relatively small masses to accelerate.

(5) The numbers of petal formation increases as the impact velocity increases but reduced in it size. At the velocity of v = 100 m/s, the impacted surface by conical nose projectile form four petals while at v = 300 m/s, five petals generated. At v = 600 m/s, seven petals formed and its size reduced. Similarly to the hemispherical nose projectile impacting target plate where the numbers of petals increases from five, six and seven petals at the velocity of 100 m/s, 300 m/s and 600 m/s, respectively.

(6) The increase of impact velocity contributes positively on the holes enlargement of perforated surface. This phenomenon occurs to all type of impact by different type of projectile nose shape including conical, hemispherical and blunt projectile. As a result, the gap between the projectile and the target also increased. The occurrence of holes expansion or enlargement is proportional with the increment of impact velocity.

(7) The influence of local strain also examined. The highest local strain generated at the point of impact between projectile and target especially at the tip of the crater which initiate crack propagation of perforated surface.

It can be concluded that the model succeeds in defining failure mechanisms associated with the configuration of projectile –target. This reinforces the hypothesis regarding the applicability of the failure criterion to capture the main aspects of the perforation process of target plate impacted by several type of projectile nose shape. Good agreement is obtained between numerical simulation, theoretical prediction and experimental results compared by others researchers. Therefore the results obtained can be used for the efficient damage of the constraints target plate under the impact of projectile. Comparison to all of projectile nose shape will eventually bring to a concise and remarkable results where the projectile nose shape were significantly influence on the failure mode profile and pattern.

Acknowledgment

This work supported by the Engineering Mechanics Department, Faculty of Mechanical and Manufacturing Engineering, Universiti Tun Hussein Onn Malaysia, Malaysia.

Nomenclature

a : Contact patch / hydrostatic core of radius
E : Young's modulus
F : Normal force
f : Failure strain
p : Mean or average contact pressure
R : Radius of curvature
ν : Poisson's ratio
ρ : Mass density
σ_y : Yield stress

References

[1] J. A. Rodriguez-Martinez, A. Rusinek, P. Chevrier, R. Bernier and A. Arias, Temperature measurements on ES steel sheets subjected to perforation by hemispherical projectiles, *Int. J. Impact Eng.,* 37 (7) (2010) 828-841.

[2] J. A. Rodriguez-Martinez, A. Rusinek, R. Pesci and R. Zaera, Experimental and numerical analysis of the martensitic transformation in AISI 304 steel sheets subjected to perforation by conical and hemispherical projectiles, *Int. J. Solids and Struct.,* 50 (2) (2013) 339-351.

[3] Z. S. Liu, S. Swaddiwudhipong and M. J. Islam, Perforation of steel and aluminum targets using a modified Johnson Cook material model, *Nuclear Eng. And Design*, 250 (0) (2012) 108-115.

[4] T. Borvik, M. J. Forrestal, O. S. Hopperstad, T. L. Warren and M. Langseth, Perforation of AA5083-H116 aluminum plates with conical-nose steel projectiles – calculations, *Int. J. Impact Eng.,* 36 (3) (2009) 426-437.

[5] M. A. Iqbal, A. Chakrabarti, S. Beniwal and N. K. Gupta, 3D numerical simulations of sharp nosed projectile impact on ductile targets, *Int. J. Impact Eng*., 37 (2) (2010) 185-195.

[6] M. A. Iqbal, S. H. Khan, R. Ansari and N. K. Gupta, Experimental and numerical studies of double nose projectile impact on aluminum plates, *Int. J. Impact Eng*., 54 (0) (2013) 232-245.

[7] W. Song, J. Ning and J. Wang, Normal impact of truncated oval-nosed projectiles on stiffened plates, *Int. J. Impact Eng*., 35 (9) (2008) 1022-1034.

[8] M. N. Ibrahim, W. A. Siswanto and A. M. A. Zaidi, Computational issues in the simulation of high speed ballistic impact: A review, *Applied Mechanics and Materials*, 315 (2013) 762-767.

[9] T. Belytschko, W. K. Liu and B. Moran, Nonlinear finite elements for continua and structure, *John Wiley*, England (2001).

[10] C. T. Lim and W. J. Stronge, Normal elastic-plastic impact in plane strain, *Mathematical and Computer Modeling*, 28 (1998) 323-340.

[11] D. Lesuer, Experimental investigation of material models for Ti-6Al-4V and 2024 T3, Lawrence Livermore National Laboratory, *U.S. Department of Energy* (1999).

[12] A. Rusinek, J. A. Rodriguez-Martinez, R. Zaera, J. R. Klepaczko, A. Arias and C. Sauvelet, Experimental and numerical study on the perforation process of mild steel sheets subjected to perpendicular impact by hemispherical projectiles, *Int. J. of Impact Eng*., 36 (4) (2009) 565-587.

[13] T. Wierzbicki, Petalling of plates under explosive and impact loading, *Int. J. Impact Eng.,* 22 (1999) 935-954.

[14] K. M. Kpenyigba, T. Jankowiak, A. Rusinek and R. Pesci, Influence of projectile shape on dynamic behavior of steel sheet subjected to impact and perforation, *Thin Walled Struct*., 65 (0) (2013) 93-104.

Mohd Norihan Ibrahim is a lecturer at Department Engineering Mechanics, Universiti Tun Hussein Onn Malaysia (UTHM). He received his bachelor degree in mechanical engineering from the University of Plymouth, UK, and completed his M.Eng (Mechanical) from UTHM and he is currently studying his Ph.D. in UTHM.